

Supporting Information: Functional colloidal micro-sieves assembled and guided above a channel-free magnetic striped film

Fernando Martinez-Perdrero,¹ Arthur V. Straube,² Tom H. Johansen,^{3,4} and Pietro Tierno^{1,5}

¹*Departament de Estructura i Constituents de la Matèria,*

Universitat de Barcelona, Avenida Diagonal 647, 08028, Barcelona, Spain

²*Department of Physics, Humboldt-Universität zu Berlin, Newtonstr. 15, D-12489 Berlin, Germany*

³*Department of Physics, The University of Oslo, P.O. Box 1048 Blindern, 0316 Oslo, Norway*

⁴*Institute for Superconducting and Electronic Materials,*

University of Wollongong, Northfields Avenue, Wollongong, NSW 2522, Australia

⁵*Institut de Nanociència i Nanotecnologia IN²UB, Universitat de Barcelona, Barcelona, Spain*

APPENDIX: THEORETICAL MODEL

1. Motion of a single particle

The motion of a single paramagnetic colloidal particle above the FGF is well explained by the interaction of the induced magnetic dipole with the non-uniform magnetic field of the FGF. A spherical particle of volume $V = (4/3)\pi a^3$ and of magnetic susceptibility χ becomes polarized in the external magnetic field \mathbf{H} , acquiring a magnetic moment $\mathbf{m} = V\chi\mathbf{H}$. The total magnetic field above the FGF \mathbf{H} is given by the superposition $\mathbf{H}^{ext} + \mathbf{H}^{sub}$ of the external modulation \mathbf{H}^{ext} and the stray field of the garnet film \mathbf{H}^{sub} .

The first contribution has the form

$$\mathbf{H}^{ext} = (H_x \cos(2\pi ft), 0, -H_z \sin(2\pi ft)). \quad (1)$$

For not very strong external fields, when the amplitude of modulation (H_0) is weak compared to the saturation magnetization (M_s), $H_0 \ll M_s$, and for the particle elevation z (i.e. the vertical distance from the center of particle to the FGF) comparable with the wavelength λ of the FGF, $z \simeq \lambda$, the stray field can be accurately approximated as [1, 2]

$$\mathbf{H}^{sub} = \frac{4M_s}{\pi} \exp\left(-\frac{2\pi z}{\lambda}\right) \left(\cos\frac{2\pi x}{\lambda}, 0, -\sin\frac{2\pi x}{\lambda}\right).$$

The energy of interaction with the field of the substrate $U = -\mu_0 \mathbf{m} \cdot \mathbf{H} = -\mu_0 V \chi (\mathbf{H}^{ext} + \mathbf{H}^{sub})^2$ taken at a fixed elevation is evaluated to yield the magnetic energy landscape

$$U(x, t) = -U_0 \left[\sqrt{1 + \beta} \cos(2\pi ft) \cos\left(\frac{2\pi x}{\lambda}\right) + \sqrt{1 - \beta} \sin(2\pi ft) \sin\left(\frac{2\pi x}{\lambda}\right) \right]. \quad (2)$$

Here, $U_0 = 8\mu_0 \chi V M_s H_0 \pi^{-1} \exp(-2\pi z/\lambda)$ is the amplitude of the potential and we have assumed that the magnetic permeability of the solvent is practically the same of that of the free space. The potential as in Eq. 2 corresponds to a running harmonic wave of an oscillating amplitude. The temporal oscillations are stronger as $|\beta| \rightarrow 1$

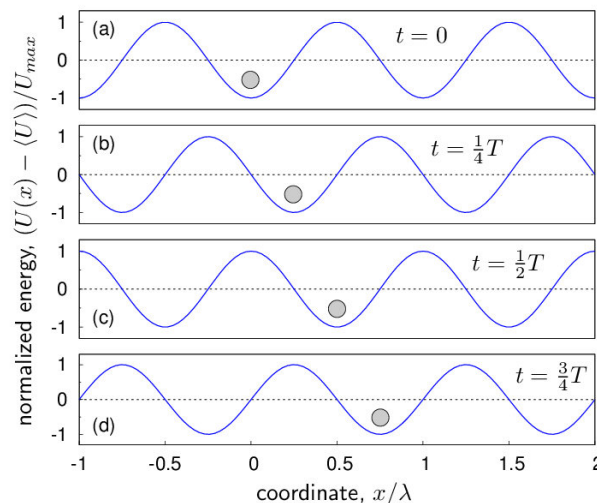


FIG. 1. Particle sitting close to a minimum of the traveling energy landscape. The energy potential corresponds to Eq. 3, which is shown at different fractions of period, $T = 1/f$: $t = 0$ (a), $t = 0.25T$ (b), $t = 0.5T$ (c), and $t = 0.75T$ (d). Moving together with the potential with the speed $v_0 = \lambda f$, after one time period the particle displaces by one wavelength λ of the landscape.

and weaker as $|\beta| \rightarrow 0$. In the case of circular polarization, $\beta = 0$, the energy landscape displays no temporal oscillations and corresponds to a sinusoidal wave of a constant amplitude U_0 which translates with a constant speed $v_0 = \lambda f$:

$$U^{(\beta=0)}(x, t) = -U_0 \cos\left(\frac{2\pi(x - v_0 t)}{\lambda}\right). \quad (3)$$

At small frequencies, the motion of an individual particle is synchronised with the potential. As a result, the particle is pinned close to an energy minimum and moves together with it with the speed v_0 , as shown in Fig. 1, which illustrates the mechanism of motion. As in Refs. [1, 3], the energy potential is shifted by the mean value and re-scaled by its maximum value. We note that at higher frequencies, the particle can lose the synchronization because the minima are moving too fast (recall that $v_0 \propto f$), its average velocity becomes smaller than

that of the potential.

2. Chain assembly

Here, we describe how a *DC* field along the stripes, in the y direction, in addition to the field rotating in the plane (x, z) can lead to the assembly of chains aligned along the stripes. Let us consider N particles numbered from 0 to $N-1$. Generally, each pair of magnetic dipoles, \mathbf{m}_l and $\mathbf{m}_{l'}$ ($l, l' = 0, \dots, N-1$ with $l' \neq l$) interacts via dipolar magnetic interactions according to the dipole-dipole potential

$$U_{dd}(\mathbf{r}_{ll'}) = \frac{\mu_0}{4\pi r_{ll'}^3} [(\mathbf{m}_l \cdot \mathbf{m}_{l'}) - 3(\hat{\mathbf{r}}_{ll'} \cdot \mathbf{m}_l)(\hat{\mathbf{r}}_{ll'} \cdot \mathbf{m}_{l'})],$$

where $\mathbf{r}_{ll'} = \mathbf{r}_l - \mathbf{r}_{l'}$ is the vector between the particles l and l' with the positions \mathbf{r}_l and $\mathbf{r}_{l'}$, $r_{ll'} = |\mathbf{r}_{ll'}|$ is the distance between the particles and $\hat{\mathbf{r}}_{ll'} = \mathbf{r}_{ll'}/r_{ll'}$ is the unit vector in the direction of $\mathbf{r}_{ll'}$.

Apart from the same elevation z , particles forming a chain aligned along a stripe have also the same x coordinates and therefore $\mathbf{r}_{ll'} = (0, y_l - y_{l'}, 0)$ possesses the y component only. Accounting for the facts that the dipoles are induced and that the field above the FGF is independent of y , we conclude that the magnetic dipoles are identical for all particles in the chain, $\mathbf{m}_l = \mathbf{m}_{l'} = \mathbf{m} = \chi V \mathbf{H}$ and the dipolar interaction potential becomes:

$$\begin{aligned} U_{dd}(\mathbf{r}_{ll'}) &= \frac{\mu_0 \chi^2 V^2}{4\pi r_{ll'}^3} [H^2 - 3H_y^2] \\ &= \frac{\mu_0 \chi^2 V^2 H^2}{4\pi r_{ll'}^3} [1 - 3\cos^2 \theta], \end{aligned} \quad (4)$$

where θ is the angle between the field \mathbf{H} and the line connecting the two particles, which is parallel to the y axis. As can be seen from Eq. 4, the vertically oriented dipoles, when $\theta = \pi/2$, $H_y = 0$, repel ($U_{dd} > 0$), while the head-to-tail orientation of the dipoles, when $\theta = 0$ and only H_y is non-vanishing, is attractive ($U_{dd} < 0$). The border case $U_{dd} = 0$ gives the neutral situation when the dipole neither repel nor attract. Setting Eq. 4 to zero, we solve the equation $1 - 3\cos^2 \theta = 0$ to obtain the ‘‘magic’’ angle, $\theta_{mag} \approx 54.7^\circ$ that the orientations with $\theta > \theta_{mag}$ and $\theta < \theta_{mag}$ lead to repulsive and attractive interactions, respectively.

The similar condition can be formulated directly in terms of the components of the magnetic field. Assuming that the dipolar interaction is mainly caused by the external modulation, as particularly confirmed by Ref. [2], we approximate $\mathbf{H} \approx \mathbf{H}^{ext}$ with \mathbf{H}^{ext} as in Eq. 1. Further, restricting our analysis by the case of circular modulation, when $\beta = 0$ and, equivalently, $H_x = H_z = H_0$, in the presence of the additional *DC* field we obtain

$$\mathbf{H} \approx (H_0 \cos(2\pi ft), H_y, -H_0 \sin(2\pi ft)). \quad (5)$$

Setting again Eq. 4 to zero and solving the equation $H^2 - 3H_y^2 = 0$ with the above expression for the field, Eq. 5, we obtain the minimal value for the *DC* field necessary to induce attractive interactions:

$$H_y^{(c)} = \frac{1}{\sqrt{2}} H_0 \approx 0.7 H_0. \quad (6)$$

Thus, for the fields $H_y < H_y^{(c)}$ the particles are repelling and the formation of chain is impossible, while for $H_y > H_y^{(c)}$ the particles attract each other and can be assembled in a chain, as shown in the main text.

3. Chain expansion

As long as the H_y component of the field is removed, the particles assembled in a chain, become repulsively interacting. Being no longer stable, the chain starts to expand. As follows from Eq. 4 for $H_y = 0$ ($\theta = \pi/2$), the dipole-dipole interaction potential of particles l and l' is strictly repulsive,

$$U_{dd}(\mathbf{r}_{ll'}) = \frac{\mu_0 \chi^2 V^2}{4\pi} \frac{H_0^2}{|\mathbf{r}_l - \mathbf{r}_{l'}|^3} = \frac{4\pi \mu_0 \chi^2 a^6 H_0^2}{9 |y_l - y_{l'}|^3}. \quad (7)$$

Here, we have taken into account that the particles in the chain have the same x and z coordinates and that $H^2 = H_0^2$ as follows from Eq. 5 at $H_y = 0$.

Considering a chain of N particles and adapting the approach by Helseth *et al.* [4], we assume that all particles in the chain remain equidistantly spaced at all times, separated by a lattice distance $d = d(t)$, we put $\mathbf{r}_l(t) = (x, y_0 + ld, z)$ with $l = 0, \dots, N-1$. Neglecting thermal fluctuations, the overdamped motion of particle l in the expanding chain can be described by the equation of motion $\zeta \dot{y}_l = -\sum_{l' \neq l} \partial_{y_l} U_{dd}(\mathbf{r}_{ll'})$, where ζ is the viscous friction coefficient. Being interested in the end-to-end distance, $\delta(t) = y_{N-1}(t) - y_0(t) = (N-1)d(t)$, we obtain a differential equation for $\delta(t)$,

$$\dot{\delta}(t) = \frac{\alpha}{\delta^4(t)}, \quad \alpha = \frac{8\pi \mu_0 \chi^2 H_0^2 a^6 (N-1)^4}{3\zeta} \sum_{l=1}^{N-1} \frac{1}{l^4}$$

Assuming that the particles touch each other at the beginning of the expansion, $t = 0$, $\delta(0) = 2a(N-1)$, we integrate the above differential equation to obtain the end-to-end distance as a function of time

$$\delta(t) = 2a(N-1) (1 + At)^{1/5} \quad (8)$$

with the coefficient

$$A = \frac{5\alpha}{32a^5(N-1)^5} = \frac{5\mu_0 \chi^2 H_0^2}{72\eta F(z)(N-1)} \sum_{l=1}^{N-1} \frac{1}{l^4}. \quad (9)$$

Here, by writing the friction coefficient between the particle and solvent as $\zeta = 6\pi\eta a F(z)$, we take account of

the wall via the function $F(z)$. If without hydrodynamic coupling to the wall $F(z) = 1$, the presence of the wall effectively modifies the friction, leading to a Faxén correction in the form

$$F^{-1}(z) \approx 1 - \frac{9}{16} \left(\frac{a}{z}\right) + \frac{1}{8} \left(\frac{a}{z}\right)^3, \quad (10)$$

as has recently been confirmed experimentally [5].

SUPPORTING MOVIES

MovieS1: motion of a magnetic chain subjected to a precessing field with the frequency $f = 3$ Hz and amplitudes $H_0 = 1000$ A/m and $H_y = 1500$ A/m. The transported colloidal cargos are non-magnetic silica particles with the diameter of $3 \mu\text{m}$, cf. Figs. 1(c) and 1(d) of the main text.

MovieS2: motion of a magnetic chain subjected to a precessing field with the frequency $f = 5$ Hz and amplitudes $H_0 = 1000$ A/m and $H_y = 2100$ A/m. Expansion of the chain is induced by switching off H_y after $t = 5.3$ s. The transported colloidal cargos are silica particles with the diameter of $3 \mu\text{m}$, cf. Figs. 2(a) and 2(d) of the main text.

MovieS3: motion of a magnetic chain subjected to a precessing field with the frequency $f = 5$ Hz and amplitudes

$H_0 = 1000$ A/m and $H_y = 1500$ A/m. The relatively high speed of the chain (12.4 m/s) allows to transport $4 \mu\text{m}$ silica spheres while smaller particles (of $1 \mu\text{m}$ size) are not trapped due to their strong thermal fluctuations.

MovieS4: a pair of chains entrapping three silica particles (of $5 \mu\text{m}$ size) after several back and forth movements. The external magnetic field has the amplitudes $H_0 = 1000$ A/m and $H_y = 1700$ A/m and frequency $f = 5$ Hz (Fig. 3 of the main text).

MovieS5: the compression of an ensemble of silica particles (of $3 \mu\text{m}$ size) by a magnetic barrier composed by two chains driven by a precessing magnetic field with the frequency $f = 1.5$ Hz and amplitudes $H_0 = 1000$ A/m and $H_y = 2100$ A/m (Fig. 4 of the main text).

-
- [1] A. V. Straube, P. Tierno, *Europhys. Lett.* **2013**, 103, 28001.
 - [2] A. V. Straube, P. Tierno, *Soft Matter* **2014**, 10, 3915.
 - [3] A. Fortini, M. Schmidt, *Phys. Rev. E* **2010**, 105, 230602.
 - [4] L. E. Helseth, H. Z. Wen, T. M. Fischer, *J. Appl. Phys.* **2006**, 99, 024909.
 - [5] J. Leach, H. Mushfique, S. Keen, R. Di Leonardo, G. Ruocco, J. M. Cooper, M. J. Padgett, *Phys. Rev. E* **2009**, 79, 026301.